

Healing Full-Thickness Cartilage Defects Using Adipose-Derived Stem Cells

JASON L. DRAGOO, M.D.,[†]* GRACE CARLSON, M.D.,* FRANK McCORMICK, M.D.,*
HAUMITH KHAN-FAROOQI, B.S.,* MIN ZHU, M.D.,*
PATRICIA A. ZUK, Ph.D.,* and PROSPER BENHAIM, M.D.*

ABSTRACT

The purpose of this study was to evaluate the use of adipose-derived stem cells (ADSCs) as a source for full-thickness cartilage repair in an animal model. Autologous ADSCs were isolated and induced with growth medium and placed in a fibrin glue scaffold and into 3-mm×4-mm full-thickness chondral defects in rabbits with negative controls. Specimens were evaluated for early healing using immunostaining, Western blotting, reverse transcriptase polymerase chain reaction, transfection with the Lac Z gene, and quantitative assessment. Twelve of 12 (100%) articular surface defects containing tissue-engineered stem cell constructs healed with hyaline-like cartilage, versus 1 of 12 (8%) in the control group ($p < .001$). There was complete healing to subchondral bone in 12 of 12 experimental defects (100%), and 10 of 12 (83%) had seamless annealing to the native cartilage. Aggrecan, superficial zone protein, collagen type II messenger ribonucleic acid, and Lac-Z gene products were identified in 12 of 12 experimental specimens, which exhibited a collagen type II:I protein ratio similar to that of normal rabbit cartilage. Quantitative histologic analysis revealed an average score of 18.2 of 21 in the experimental group, compared with 10.0 in the controls ($p = .001$). Induced ADSCs supported in a fibrin glue matrix are a promising cell source for cartilage tissue engineering.

INTRODUCTION

ARTICULAR CARTILAGE is a narrow layer of highly specialized connective tissue that permits smooth, nearly frictionless movement and load-bearing force dispersal throughout the joint. When this tissue is disrupted, resulting in a full-thickness defect, little healing occurs.¹ Defects measuring 10 mm and larger lead to significant stress concentration on the surrounding cartilage and to arthritic degeneration.² This altered load distribution has important implications relating to the long-term integrity of cartilage

adjacent to chondral defects. Thus, large osteochondral defects are accepted indications for surgical intervention if the patient is symptomatic.

Current surgical strategies rely on the production of fibrocartilage using bone marrow stimulation techniques, such as microfracture and abrasion arthroplasty, or the transfer of osteochondral grafts from a nearby area of the articular surface. Because the lack of resiliency of fibrocartilage or donor site morbidity hamper the outcomes of these procedures, recent research has focused on tissue-engineered hyaline-like cartilage.³⁻⁶

[†]Orthopedic Tissue Regeneration Laboratory, Department of Orthopedic Surgery, Stanford University School of Medicine, Palo Alto, California; and *Laboratory for Regenerative Bioengineering and Repair, Department of Orthopedic Surgery, UCLA School of Medicine, Los Angeles, California.

Chondrocytes or stem cells are required to produce tissue-engineered cartilage. Chondrocytes appear to retain zonal memory, which may be problematic if a superficial zone cell is seeded into the deep zone layer.⁷ Many laboratories have focused on the use of stem cells for cartilage engineering, because they are easy to culture and do not require zonal seeding.^{8,9}

Human liposuction aspirates contain multipotent cells, otherwise known as adipose-derived stem cells (ADSCs). Isolation of several single-cell cloned populations has shown that they possess at least a tri-lineage potential to differentiate into fat, bone, and cartilage.^{10,11} These ADSCs have been induced into cartilage *in vitro* and *in vivo*.^{10–13} Human ADSCs are easier to obtain, have lower donor-site morbidity, and are available in larger numbers than stem cells harvested using bone marrow aspiration.^{10,11,14,15} Obtaining large numbers of stem cells at harvest may eliminate the need for costly and lengthy tissue-culture expansion. Additionally, a variety of specialists can perform the fat harvest procedure using liposuction, arthroscopy, or subcutaneous fat biopsy.^{11,12}

Previous studies have shown hyaline-like cartilage formation after subcutaneous implantation of an ADSC nodule into an animal model.¹² The purpose of this study was to evaluate the ability of ADSCs to heal full-thickness cartilage defects in an animal model.

MATERIALS AND METHODS

Isolation of progenitor cells

After approval from the Animal Research Committee at the University of California, Los Angeles, parascapular adipose tissue was obtained from 12 6-month-old, 9-pound New Zealand White Rabbits. ADSCs were extracted from the lipoaspirate solution using a previously published protocol.¹⁰ Briefly, after the fat underwent a series of washes with phosphate (PBS) saline, it was digested with 0.075% collagenase (Sigma, St. Louis, MO) at 37°C for 45 min. The supernatant was removed along with the mature adipocytes, leaving the ADSC solution. After neutralization of the collagenase with 10% fetal bovine serum (FBS, Tissue Culture Biologics, Tulare, CA), the cell solution was centrifuged at 5000 rpm for 6 min. The supernatant was again discarded to isolate the ADSCs. The resultant cellular fraction containing ADSCs was resuspended in Delbecco's modified Eagle medium with 10% FBS (DMEM-10, Cellgro, Herdon, VA). The cellular yield was calculated using a hemacytometer, and cell viability was checked using trypan blue exclusion dye. Cells were expanded in culture medium (DMEM/F-12 1:1; Life Technologies, Grand Island, NY) supplemented with 10% FBS and 1% antibiotic/antimycotic (10,000 units/mL penicillin G, 25 µg/mL amphotericin B, 10,000 µg/mL streptomycin; Cellgro, Herdon, VA). When the cells reached 90% confluence, the cultures were trypsinized (0.125% trypsin (Life Technologies) and were subcultured for 2 passages on 75-cm³ cultured flasks (BD Bioscience, San Jose, CA).

Lac-Z virus transfection

Each experimental group was standardized for cell number using a hemocytometer and trypan blue exclusion. Development of recombinant adenovirus with lac-Z (Ad-lac-Z) was achieved by inserting the complementary deoxyribonucleic acid (cDNA) for recombinant lac-Z into the plasmid vector pAC-cytomegalovirus. The plasmid was then transfected into 293 cells, an embryonal renal cell line that is highly permissive to adenovirus transduction. Plaques containing recombinant adenovirus (Ad-lac-Z) were then purified, propagated, and titered in 293 cells. When cultures reached 90% confluence, appropriate cultures were transduced with Ad-lac-Z. Three mL of DMEM-10 was added to the plates chosen for transduction. Virus was added at a multiplicity of infection of 100. The plates were then incubated at 37°C and stirred occasionally for 1 h. An additional 7 mL of DMEM-10 was added to each plate, and incubation was continued for 24 h. The supernatant was removed, and a small number of the cells were analyzed for the expression of β-galactosidase (gene product of lac-Z) to confirm the transfection process. The cells were fixed in 4% paraformaldehyde for 10 min at room temperature. The cells were washed with PBS and incubated for 1 h with a polyclonal mouse antibody specific to β-galactosidase (Biomedica, Foster City, CA). After incubation, the cells were washed in PBS, and the antibody-β-galactosidase conjugate was detected using a biotin-streptavidin-horseradish peroxidase (HRP) detection system (VectaStain RTU kit, Vector Laboratories, Burlingame, CA) according to the manufacturer. The remainders of the transduced cells were induced and implanted using the same techniques as for the nontransduced cells. The analysis of 6-week specimen sections was performed using the above technique.

Chondrogenic induction

After the ADSCs were expanded, they were prepared for an autologous graft. After the cells reached confluence, micromasses of cartilage were created by plating 25 microliters of 2×10^7 cells/cm³ into well culture plates. After incubation for 2 h, cells were given 0.25 mL of chondrogenic medium consisting of DMEM/F-12 1:1, 10% FBS, 1% antibiotic/antimycotic, 100 ng/mL of insulin-like growth factor-1, 5 ng/mL of fibroblast growth factor-2, 10 ng/mL of growth hormone, 5 ng/mL of transforming growth factor-beta, 50 µg/mL of ascorbic acid-2 phosphate, and 6.25 µg/mL of transferrin. Cells were incubated at 37°C at 5% carbon dioxide, and chondrogenic medium was changed after the first 24 h and every 48 h thereafter for 2 weeks. The micromass cells were then broken apart with 0.025% collagenase and resuspended in autologous fibrin glue at a concentration of 1.5×10^7 cells/cm³. 300 µl of cell suspension was then formed into a nodule, as shown in Figure 1, by adding 30 µL of thrombin (3000 U/mL)/calcium carbonate (40 mM) solution at a 1:4 ratio to

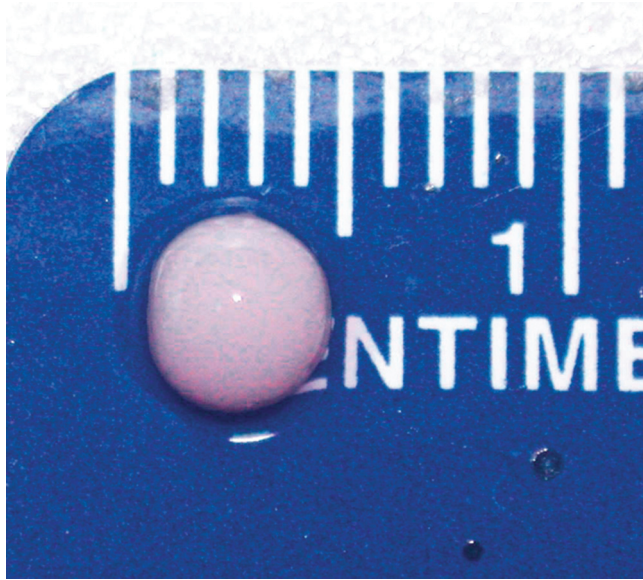


FIG. 1. Cartilage-stem cell nodule before implantation into animal. Color images available online at www.liebertpub.com/ten.

coagulate. Cells were then cultured *in vitro* for another 7 days in chondrogenic media.

Animal implantation

Twelve 6-month-old male, 9-pound New Zealand rabbits were anesthetized, and bilateral medial parapatellar incisions were made to expose the medial femoral condyles. A 3-mm- \times 4-mm-deep full-thickness articular surface defect was made in the weight-bearing surface of the medial femoral condyle of each knee using a dermal punch. A 3-mm defect was chosen because it is the largest fully constrained (bordered by normal articular cartilage on all sides) defect possible on the medial femoral condyle of adult rabbits, and negative control lesions did not heal in pilot studies (data not shown). The cartilage surface was punched until the calcified cartilage layer was reached. A cylinder of cartilage was then removed measuring approximately 3 mm \times 4 mm. The depth varied slightly because of differences in cartilage thickness. The base of the defect was then curetted to remove any remaining cartilage. Autologous fibrin glue was then used to seal the subchondral bone and minimize contamination of marrow cells and act as an adhesive for the nodule. The autologous ADSC nodule was then press-fit into the defect and recessed 1 mm below the articular surface to avoid early shear stresses during the healing process. The contralateral control lesion was left empty. Postoperatively, the rabbits were allowed full weight bearing and were killed at 8 weeks. The areas of defect repair were excised, and histological samples were prepared.

Analysis of cartilage

All specimens were analyzed grossly.

Histochemical staining

After the specimens had been fixed in paraformaldehyde and embedded in paraffin, 6- μ m sections were cut, mounted on slides, and stained using standard hematoxylin and eosin, Alcian blue (at pH 1), and β -galactosidase biotin-streptavidin-HRP staining protocols. Digital images were obtained using a Zeiss Axioskop II microscope (Carl Zeiss, Munich, Germany) and Spot software (Diagnostic Instruments Inc., Sterling Heights, MI).

Quantitative histologic analysis

Histologic grading was performed using the modified histologic scoring system of Moran¹⁶ that evaluated nature, surface thickness, integrity, bonding, and absence of degenerative changes. This scale was modified to substitute Alcian blue staining (pH 1) for Safranin-O staining.

Immunohistochemical staining

Paraffin sections were deparaffinized in xylene and then hydrated in decreasing ethanol solutions (100% to 70%). Sections were predigested for 1 h at 37°C in 0.5 mL of chondroitinase avidin-biotin complex in 50 mM Tri-hydrochloride buffer (pH 8.0) containing 30 mM sodium acetate, 0.5 mg/mL bovine serum albumin, and 10 mM N-ethylmaleimide. Endogenous peroxidase activity was quenched by incubation with 3% hydrogen peroxide for 15 min. Non-specific binding was blocked by incubation in PBS with 10% horse serum. The sections were incubated for 1 h at 37°C in PBS with 10% horse serum containing primary antibodies to collagen type II. Antigen-antibody complexes were detected with the Vectastain ABC kit (Vector Laboratories) according to instructions provided by the manufacturer.

Ribonucleic acid/gene expression using reverse transcriptase polymerase chain reaction

Conventional reverse transcriptase polymerase chain reaction (RT-PCR) was performed using the Eppendorf Master Mix (Eppendorf, Westbury, NY). Each reaction (25 μ L final volume) contained the following: cDNA (10% of final PCR reaction volume), 5 μ M each of a forward and reverse primer (Operon—Fisher Scientific; for primer sequences, see Supplemental Table S1), XX units of master mix, and the appropriate volumes of provided PCR buffer. Each reaction was amplified for 40 cycles at 53°C. The PCR reactions were resolved using conventional agarose gel electrophoresis. RT-PCR reactions containing primers to human β -actin were also run as an internal control. For PCR/real-time amplification of the cDNA, we used primer pairs designed to the following genes: (F = forward oligo, R = reverse oligo).

(a) Human collagen type II α 1

(expected product size: 328 bp)

F = 5'-CCA AGT ACT TTC CAA TCT CAG TCA C-3'

R = 5'-ACA GAA TAG CAC CAT TGT GTA GGA C-3'

(b) Human collagen type I
(expected product size: 598 bp)
 $F = 5'$ -CAT CTC CCC TTC GTT TTT GA-3'
 $R = 5'$ -CTG TGG AGG AGG GTT TCA GA-3'

(c) Aggrecan
(expected product size: 500 bp)
 $F = 5'$ -GCG ATA TCA TGA CCA CTT TAC TC-3'
 $R = 5'$ -CCT GTC AAA GTC GAG GGT GT-3'

(d) Superficial Zone Protein
 $F = 5'$ -GGAGATGTGGGAAGGGTAT-3'
 $R = 5'$ -GAAGAGGAGGAGGAGGAGGA-3'

Real-time PCR

For real-time PCR, cDNA was synthesized using Taqman Gold reagents (Applied Biosystems, Foster City, CA). Reactions were performed using the Quantitect Probe PCR Kit (Qiagen, Valencia, CA), which were run in an ABI7700 analyzer (Applied Biosciences, Foster City, CA). Expression of the housekeeping gene glyceraldehyde-3 phosphate dehydrogenase (GAPDH) was also run as a normalization control for all real-time PCR reactions.

Quantitated Western blot

ADSC populations were maintained in until 80% confluent. The cells were washed in PBS and lysed in a standard RIPA buffer (150 mM sodium chloride, 50 mM Tris-chloride pH 7.4, 0.5% sodium deoxycholate, 0.1% sodium dodecyl sulfate, 1.0% TX-100, 1 mM phenylmethanesulphonyl fluoride, and 5 µg/mL each aprotinin and leupeptin). Equivalent amounts of ASC and AOC lysates were analyzed using conventional Western blotting protocols for nitrocellulose filters. Filters were blocked and incubated with the indicated antibodies at their recommended dilutions in Western Blocking Buffer (WBB; PBS, 5% powdered milk, 0.1% Tw-20). Proteins were detected using HRP-conjugated secondary antibodies according to the manufacturer (Bio-Rad, Hercules, CA) and the HRP enzyme developed using standard chemiluminescent reagents. Protein expression was normalized GAPDH, and expression levels were quantitated using conventional densitometry (J Image Software, NIH, Bethesda, MD). Ratio of collagen type II to type I was then calculated.

Statistics

Statistics for histologic analysis was completed using a Fisher exact test analysis, using $p = .05$ as the significance level.

RESULTS

Laboratory preparation of the stem cell nodules demonstrated a rubbery, translucent, whitish appearance before



FIG. 2. Healed medial femoral defect 6 weeks after implantation. Successful integration into surrounding native cartilage. Color images available online at www.liebertpub.com/ten.

implantation in the animal (Fig. 1). All 24 specimens were harvested successfully. All 12 (100%) articular surface defects containing tissue-engineered stem cell constructs completely healed under macroscopic evaluation, versus 1 of 12 (8%) in the control group ($p < .001$). The tissue-engineered cartilage was rubbery in consistency, with a uniformly semi-transparent white color and smooth, gliding surface, similar to adjacent native cartilage (Fig. 2). The controls had little to no healing under macroscopic evaluation, with shallow, irregular regenerate tissue resembling thin fibrous tissue (Fig. 3).

Hematoxylin and eosin staining of the experimental group demonstrated complete healing to the subchondral bone in 12 of 12 experimental defects (100%), and 10 (83%) had seamless annealing of the nodule to the native cartilage in multiple sections (Fig. 4); whereas 2 (17%) exhibited minor fissuring. This is in contrast to the control group, in which 0

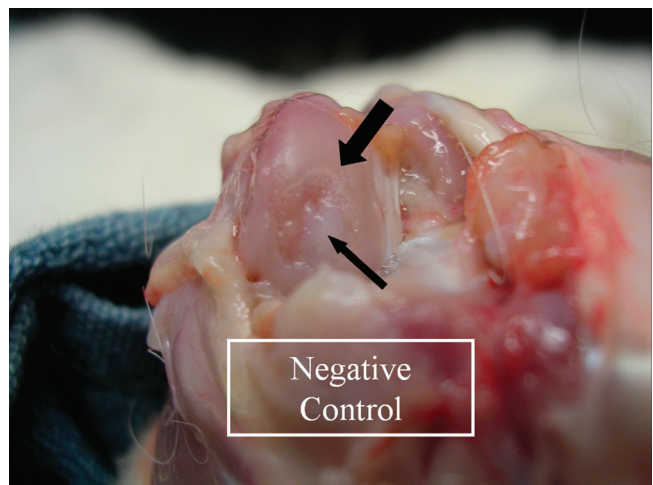


FIG. 3. Negative control showing poor restoration of articular surface. Color images available online at www.liebertpub.com/ten.



FIG. 4. Hematoxylin and eosin micrograph of healed defect at 6 weeks. Complete integration into surrounding cartilage and subchondral bone. Arrows and dotted lines indicate margins of original chondral defect. Color images available online at www.liebertpub.com/ten.

of 12 had seamless annealing to the native cartilage, 1 of 12 (8%) had minor fissuring, and 11 of 12 (92%) had major fissuring. Formation of a tangential-like superficial layer was seen in 12 of 12 (100%) experimental specimens, although a recognizable tidemark was present in 0 of 12 (Fig. 4). An independent pathologist graded the histology as hyaline cartilage architecture (minus tidemark) in 11 of 12 (92%) and hyaline-like cartilage (fibro-hyaline) in 1 of 12 (8%) experimental specimens. The control group was graded as fibrocartilage in 12 of 12 (100%) specimens (Fig. 5) ($p < .001$).

Using quantitative histologic analysis with a modified Moran score,¹⁶ the experimental tissue engineered group had an average score of 18.2 of 21, compared with an average score of 10 of 21 for controls ($p = .001$). Staining with Alcian blue was positive in 12 of 12 experimental specimens, confirming sulfated proteoglycan expression within the cellular matrix (Fig. 6). Twelve of 12 tissue-engineered specimens immunostained positive for collagen type II, whereas 1 of 12 negative controls possessed minimal staining, and 11 of 12 contained no staining (Fig. 7) ($p < .001$). Twelve of 12 experimental group specimens stained positive for the lac-Z gene and 0 of 12 controls stained positive, indicating that the tissue-engineered cartilage was composed mostly of ADSCs (Fig. 8) ($p < .001$).

RT-PCR analysis confirmed the presence of collagen type II, aggrecan, and superficial zone protein mRNA in 12 of 12 specimens (Fig. 9). The product of PCR positive controls was of proper base pair size, whereas negative controls



FIG. 5. Negative control demonstrating minimal healing with fibrocartilage. Color images available online at www.liebertpub.com/ten.

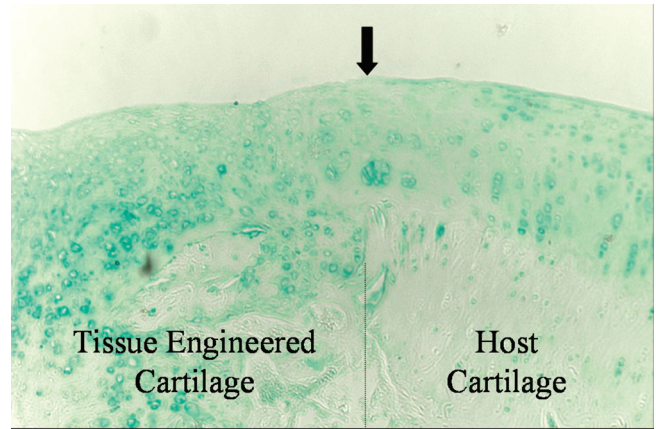


FIG. 6. Alcian blue staining (pH 1) at junction of native and tissue-engineered cartilage. Arrow and dotted line demonstrate edge of experimental defect. Color images available online at www.liebertpub.com/ten.

remained negative. Quantitative RT-PCR demonstrated a 3.14 ± 1.40 fold increase in aggrecan mRNA in the experimental group compared to the negative controls. Positive controls exhibited a 5.21 ± 0.090 fold increase in aggrecan mRNA compared to the experimental group. Type II collagen mRNA in the experimental group was 2.30 ± 0.275 times greater than in negative controls and 13.82 ± 0.0048 than in the positive controls.

Western blotting normalized to GAPDH and quantified using standard densitometry demonstrated a 19% higher collagen type II:I protein ratio than with normal rabbit articular cartilage and a 57% higher ratio than negative controls

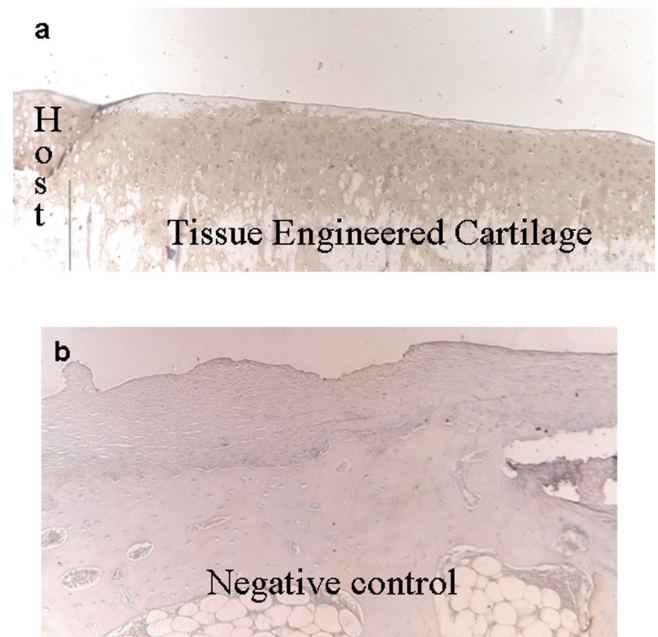


FIG. 7. Collagen type II immunostaining of (A) stem cell repair and (B) negative control. Color images available online at www.liebertpub.com/ten.

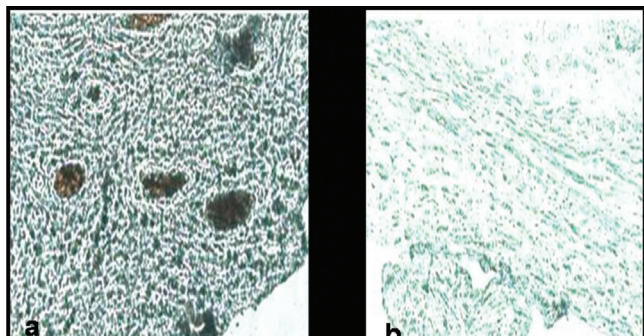


FIG. 8. High-power micrograph of lac-Z staining after transfection of stem cells with lac-Z gene. (A) Stem cell repair is mostly composed of transfected ADSCs. (B) Negative control with no lac-Z present. Color images available online at www.liebertpub.com/ten.

(Fig. 10) (Table 1). Collagen type II protein levels in the tissue-engineered specimens were 31% higher than positive controls and 65% higher than in negative controls. Collagen type I protein levels in the tissue-engineered specimens were 16% higher than in positive controls and 18% higher than in negative controls.

DISCUSSION

Gross histologic and biochemical analysis indicated that induced ADSCs supported in a fibrin glue matrix are a prom-

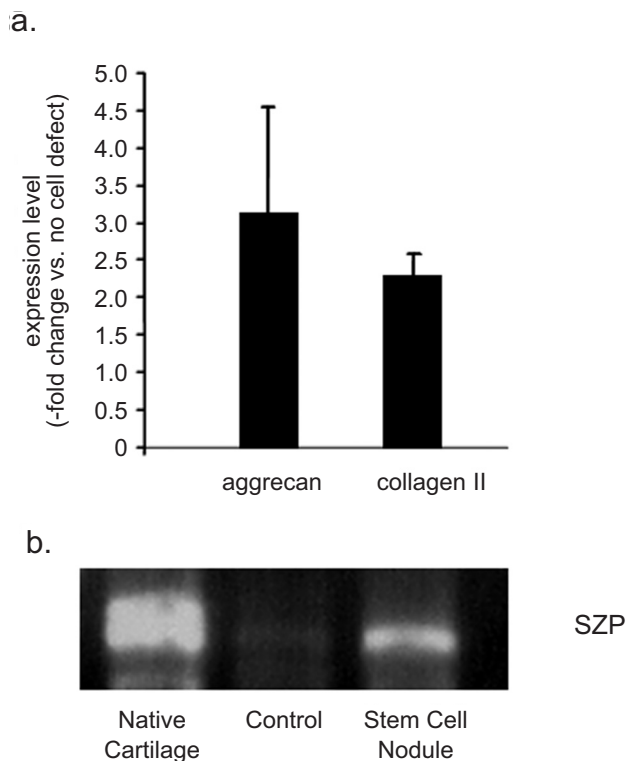


FIG. 9. Polymerase chain reaction. SZP, superficial zone protein.

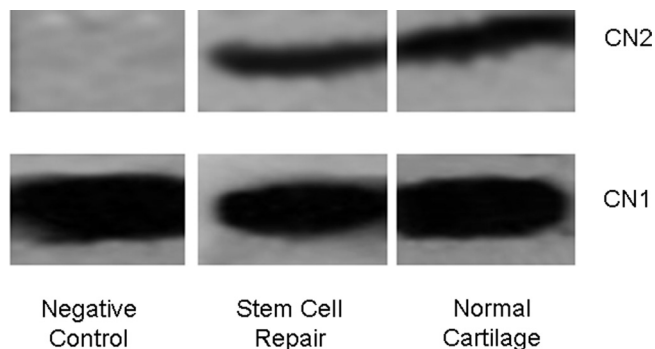


FIG. 10. Western blotting normalized to glyceraldehyde-3 phosphate dehydrogenase. CN2, collagen type II; CN1, collagen type I.

ising cell source for autologous cartilage regeneration. Upon macroscopic inspection, it appeared that the implanted stem cells developed the early functional characteristics of native hyaline cartilage, demonstrating a smooth gliding surface with a pearly semitransparent color and a smooth, rubbery consistency.

Histologic analysis also supported early chondrogenic induction, with hematoxylin and eosin staining strongly resembling the structural characteristics of immature hyaline cartilage. All nodules showed complete integration into the subchondral bone, which is necessary for implant stabilization and resistance to shear forces within the joint. The integration of the graft into surrounding cartilage was also promising. This has been a limitation with other non-stem cell-based strategies, especially with the use of mature chondrocytes.¹⁷ The presence of superficial zone protein in the grafts, along with histologic evidence of formation of a tangential-like layer, also suggests remodeling of the grafts to withstand shear forces *in vivo*.

Twelve of 12 defects stained positive for Alcian blue, which is specific for highly sulfated proteoglycans, which are a major component of hyaline cartilaginous extracellular matrix. Immunostaining for collagen type II was also positive, indicating specific collagen production of the hyaline cartilage phenotype. The ratio of collagen type II:I of the experimental group was similar to that of native articular cartilage, which indicates the production of hyaline, or hyaline-like, cartilage.

However, the lack of a recognizable tidemark under the tissue-engineered cartilage may make the grafts susceptible

TABLE 1. QUANTIFIED WESTERN BLOT NORMALIZED TO GAPDH

Assay	Stem Cell Repair	Negative Control	Native Cartilage
Collagen Type I	2.89	2.36	2.44
Collagen Type II	1.56	0.54	1.08
Collagen II/I Ratio	0.54	0.23	0.44

to long-term degeneration. Alternative engineering strategies such as composite grafting or longer-term healing may be necessary to create the calcified cartilage layer.¹⁸

The use of ADSCs as a source for autologous cartilage defect repair is promising, although further investigation is necessary. Longer-term analysis of the tissue-engineered cartilage will determine whether it is biomechanically strong enough to withstand the compressive and shear forces experienced *in vivo*. An additional study focusing on the biomechanical properties of the tissue-engineered cartilage is also necessary. Fibrin glue matrices appear to promote good hyaline histology with the use of ADSCs, although they may not possess enough integrity to support the healing of larger defects. A second, more-rigid matrix may be required for larger, unconstrained defects. Lastly, a study comparing current clinical techniques, such as microfracture and mosaicplasty, with this tissue-engineering technique must be completed.

ADSCs appear to be a useful stem cell population for tissue-engineered cartilage regeneration when used with appropriate induction signals and a fibrin glue matrix. Adipose tissue is an attractive source because of its abundance in the body, limited donor-site morbidity, and ease of harvesting.

REFERENCES

- Mankin, H.J. Current concepts review: the response of articular cartilage to injury. *J Bone Joint Surg Am* **62A**, 460, 1982.
- Guettler, J.H., Demetropoulos, C.K., Yang, K.H., and Jurist, K.A. Osteochondral defects in the human knee: influence of defect size on cartilage rim stress and load redistribution to surrounding cartilage. *J Am Sports Med* **32**, 1451, 2004.
- Buckwalter, J.A., and Mankin, H.J. Articular cartilage repair and transplantation. *Arthritis Rheum* **41**, 1331, 1998.
- Buckwalter, J.A., Mow, V.C., and Ratcliffe, A. Restoration of injured or degenerated articular cartilage. *J Am Acad Orthop Surg* **2**, 192, 1994.
- Jackson D.W., Scheer, M.J., and Simon, T.M. Cartilage substitutes: overview of basic science and treatment options. *J Am Acad Orthop Surg* **9**, 37, 2001.
- O'Driscoll, S.W. Current concepts review: the healing and regeneration of articular cartilage. *J Bone Joint Surg Am* **80A**, 1795, 1998.
- Grande D.A., Breitbart A.S., Mason J., Paulino C., Laser J., Schwartz R.E. Cartilage tissue engineering: current limitations and solutions. *Clin Orthop Relat Res* **367 Suppl**, S176, 1999.
- Gimble, J.M. Adipose tissue-derived therapies. *Expert Opin Biol Ther* **3**, 705, 2003.
- Guilak F., Awad H.A., Fermor, B., Leddy, H.A., and Gimble, J.M. Adipose-derived adult stem cells for cartilage tissue engineering. *Biorheology* **41**, 389, 2004.
- Zuk, P.A., Zhu, M., Ashjian P., De Ugarte D.A., Huang, J.I., Minzuno, H., Alfonzo Z.C., Fraser, J.K., Benhaim, P., and Hedrick, M.H. Human adipose tissue is a source of multipotent stem cells. *Mol Biol Cell* **13**, 4279, 2002.
- Zuk, P.A., Zhu, M., Minzuno, H., Huang, J., Futrell, J.W., Katz, A.J., Benhaim, P., Lorenz, H.P., and Hedrick, M.H. Multilineage cells from human adipose tissue: implications for cell-based therapies. *Tissue Eng* **7**, 211, 2001.
- Dragoo, J.L., Samimi, B., Zhu, M., Hame S.L., Thomas, B.J., Lieberman, J.R., Hedrick, M.H., and Benhaim, P. Tissue-engineered cartilage and bone using stem cells from human infrapatellar fat pads. *J Bone Joint Surg Br* **85B**, 740, 2003.
- Huang, J.I., Zuk, P.A., Jones, N.F., Zhu, M., Lorenz, H.P., Hedrick, M.H. and Benhaim, P. Chondrogenic potential of multipotential cells from human adipose tissue. *Plast Reconstr Surg* **113**, 585, 2004.
- De Ugarte, D.A., Morizono, K., Elbarbary, A., Alfonzo, Z., Zuk, P.A., Zhu, M., Dragoo, J.L., Ashjian, P., Thomas, B., Benhaim, P., Chen, I., Fraser, J., Hedrick, M.H. Comparison of multi-lineage cells from human adipose tissue and bone marrow. *Cells Tissues Organs* **174**, 101, 2003.
- Nathan, S., Das, De S., Thambyah, A., Fen, C., Goh, J., and Lee, E.H. Cell-based therapy in the repair of osteochondral defects: a novel use for adipose tissue. *Tissue Eng* **9**, 733, 2003.
- Moran, M.E., Kim, H.K., and Salter, R.B. Biological Resurfacing of full-thickness defects in patellar articular cartilage of the rabbit. Investigation of autogenous periosteal grafts subject to continuous passive motion. *J Bone Joint Surg Br* **74B**, 659, 1992.
- Schreiber, R.E., Ilten-Kirby, B.M., Dunkelman, N.S., Symons, K.T., Rekettye, L.M., Willoughby, J., and Ratcliffe, A. Repair of osteochondral defects with allogeneic tissue engineered cartilage implants. *Clin Orthop Relat Res* **367 Suppl**, S382, 1999.
- Shao, X., Goh, J.C., Hutmacher, D.W., Lee, E.H., and Zigang, G. Repair of large articular osteochondral defects using hybrid scaffolds and bone marrow-derived mesenchymal stem cells in a rabbit model. *Tissue Eng* **12**, 1539, 2006.

Address reprint requests to:

Jason L. Dragoo, M.D.

Assistant Professor

Stanford University

Department of Orthopedic Surgery

Sports Medicine Division

1000 Welch Road

Stanford, CA 94304

E-mail: jdragoo@stanford.edu